

Supplement of Geosci. Model Dev., 13, 2379–2392, 2020
<https://doi.org/10.5194/gmd-13-2379-2020-supplement>
© Author(s) 2020. This work is distributed under
the Creative Commons Attribution 4.0 License.



Supplement of

An online emission module for atmospheric chemistry transport models: implementation in COSMO-GHG v5.6a and COSMO-ART v5.1-3.1

Michael Jähn et al.

Correspondence to: Dominik Brunner (dominik.brunner@empa.ch)

The copyright of individual parts of the supplement might differ from the CC BY 4.0 License.

S1 Temporal profiles

The time profiles of emissions were originally published by TNO for SNAP emission categories (Denier van der Gon et al., 2011; Pouliot et al., 2012) and have been mapped to GNFR categories within the CHE project (Hausaissa et al., 2018).

Table S1. Emission temporal profiles for month-of-year as a function of the GNFR category.

GNFR Category	Jan	Feb	Mar	Apr	May	Jun	Jul	Aug	Sep	Oct	Nov	Dec
A Public Power	1.2	1.15	1.05	1	0.9	0.85	0.8	0.875	0.95	1	1.075	1.15
B Industry	1.1	1.075	1.05	1	0.95	0.9	0.93	0.95	0.97	1	1.025	1.05
C Other Stationary Combustion	1.7	1.5	1.3	1	0.7	0.4	0.2	0.4	0.7	1.05	1.4	1.65
D Fugitives	1.2	1.2	1.2	0.8	0.8	0.8	0.8	0.8	0.8	1.2	1.2	1.2
E Solvents	0.95	0.96	1.02	1	1.01	1.03	1.03	1.01	1.04	1.03	1.01	0.91
F Road Transport	0.88	0.92	0.98	1.03	1.05	1.06	1.01	1.02	1.06	1.05	1.01	0.93
G Shipping	1	1	1	1	1	1	1	1	1	1	1	1
H Aviation	1	1	1	1	1	1	1	1	1	1	1	1
I Off Road	1	1	1	1	1	1	1	1	1	1	1	1
J Waste	1	1	1	1	1	1	1	1	1	1	1	1
K Agricultural Livestock	0.7	0.75	0.85	0.9	1	1.1	1.2	1.25	1.3	1.1	1	0.85
L Agricultural Other	0	2	4.75	2.9	0.5	0.4	0.2	0.5	0.75	0	0	0

Table S2. Emission temporal profiles for day-of-week as a function of the GNFR category.

GNFR Category	Mon	Tue	Wed	Thu	Fri	Sat	Sun
A Public Power	1.06	1.06	1.06	1.06	1.06	0.85	0.85
B Industry	1.08	1.08	1.08	1.08	1.08	0.8	0.8
C Other Stationary Combustion	1.08	1.08	1.08	1.08	1.08	0.8	0.8
D Fugitives	1	1	1	1	1	1	1
E Solvents	1.2	1.2	1.2	1.2	1.2	0.5	0.5
F Road Transport	1.02	1.06	1.08	1.1	1.14	0.81	0.79
G Shipping	1	1	1	1	1	1	1
H Aviation	1	1	1	1	1	1	1
I Off Road	1	1	1	1	1	1	1
J Waste	1	1	1	1	1	1	1
K Agricultural Livestock	1	1	1	1	1	1	1
L Agricultural Other	1	1	1	1	1	1	1

Table S3. Emission temporal profiles for hour-of-day (first 12 hours) as a function of the GNFR category.

GNFR Category	1	2	3	4	5	6	7	8	9	10	11	12
A Public Power	0.79	0.72	0.72	0.71	0.74	0.8	0.92	1.08	1.19	1.22	1.21	1.21
B Industry	0.75	0.75	0.78	0.82	0.88	0.95	1.02	1.09	1.16	1.22	1.28	1.3
C Other Stationary Combustion	0.38	0.36	0.36	0.36	0.37	0.5	1.19	1.53	1.57	1.56	1.35	1.16
D Fugitives	1	1	1	1	1	1	1	1	1	1	1	1
E Solvents	0.5	0.35	0.2	0.1	0.1	0.2	0.75	1.25	1.4	1.5	1.5	1.5
F Road Transport	0.19	0.09	0.06	0.05	0.09	0.22	0.86	1.84	1.86	1.41	1.24	1.2
G Shipping	1	1	1	1	1	1	1	1	1	1	1	1
H Aviation	1	1	1	1	1	1	1	1	1	1	1	1
I Off Road	1	1	1	1	1	1	1	1	1	1	1	1
J Waste	1	1	1	1	1	1	1	1	1	1	1	1
K Agricultural Livestock	1	1	1	1	1	1	1	1	1	1	1	1
L Agricultural Other	1	1	1	1	1	1	1	1	1	1	1	1

Table S4. Emission temporal profiles for hour-of-day (last 12 hours) as a function of the GNFR category.

GNFR Category	13	14	15	16	17	18	19	20	21	22	23	24
A Public Power	1.17	1.15	1.14	1.13	1.1	1.07	1.04	1.02	1.02	1.01	0.96	0.88
B Industry	1.22	1.24	1.25	1.16	1.08	1.01	0.95	0.9	0.85	0.81	0.78	0.75
C Other Stationary Combustion	1.07	1.06	1	0.98	0.99	1.12	1.41	1.52	1.39	1.35	1	0.42
D Fugitives	1	1	1	1	1	1	1	1	1	1	1	1
E Solvents	1.5	1.5	1.5	1.5	1.5	1.4	1.25	1.1	1	0.9	0.8	0.7
F Road Transport	1.32	1.44	1.45	1.59	2.03	2.08	1.51	1.06	0.74	0.62	0.61	0.44
G Shipping	1	1	1	1	1	1	1	1	1	1	1	1
H Aviation	1	1	1	1	1	1	1	1	1	1	1	1
I Off Road	1	1	1	1	1	1	1	1	1	1	1	1
J Waste	1	1	1	1	1	1	1	1	1	1	1	1
K Agricultural Livestock	1	1	1	1	1	1	1	1	1	1	1	1
L Agricultural Other	1	1	1	1	1	1	1	1	1	1	1	1

S2 Vertical profiles

Vertical profiles are based on source-specific profiles developed for the European Monitoring and Evaluation Program (EMEP) (Bieser et al., 2011) that have been modified for the SMARTCARB project (Brunner et al., 2019).

Table S5. Vertical profile of the distribution of emissions as a function of the GNFR category.

GNFR Category	20m	92m	184m	324m	522m	781m	1106m
A Public Power	0	0	0.0025	0.51	0.453	0.0325	0.002
B Industry	0.06	0.16	0.75	0.03	0	0	0
C Other Stationary Combustion	1	0	0	0	0	0	0
D Fugitives	0.02	0.08	0.6	0.3	0	0	0
E Solvents	1	0	0	0	0	0	0
F Road Transport	1	0	0	0	0	0	0
G Shipping	0.2	0.8	0	0	0	0	0
H Aviation	0.25	0.25	0.1	0.1	0.1	0.1	0.1
I Off Road	1	0	0	0	0	0	0
J Waste	0	0	0.41	0.57	0.02	0	0
K Agricultural Livestock	1	0	0	0	0	0	0
L Agricultural Other	1	0	0	0	0	0	0

S3 COSMO-GHG example namelist INPUT_GHG

```
&GHGCTL
  in_tracers = 1,
/
5 &TRACER
  yshort_name = "CO2_ALL",
  itype_emiss = 2,
  itype_tscale = 1,
10 ycat1 = "CO2_A_TNO","CO2_B_TNO","CO2_C_TNO","CO2_F1_TNO","CO2_F2_TNO",
          "CO2_F3_TNO","CO2_D_TNO","CO2_E_TNO","CO2_G_TNO","CO2_H_TNO",
          "CO2_I_TNO","CO2_J_TNO","CO2_K_TNO","CO2_L_TNO","CO2_B_Carbocount",
          "CO2_C_Carbocount","CO2_J_Carbocount","CO2_L_Carbocount",
          "CO2_F_Carbocount"
15 ytpl = "GNFR_A_TNO","GNFR_B_TNO","GNFR_C_TNO","GNFR_F_TNO","GNFR_F_TNO",
          "GNFR_F_TNO","GNFR_D_TNO","GNFR_E_TNO","GNFR_G_TNO","GNFR_H_TNO",
          "GNFR_I_TNO","GNFR_J_TNO","GNFR_K_TNO","GNFR_L_TNO","GNFR_B_Carbocount"
          "GNFR_C_Carbocount","GNFR_J_Carbocount","GNFR_L_Carbocount",
          "GNFR_F_Carbocount",
20 yvpl = "GNFR_area_sources","GNFR_area_sources","GNFR_area_sources",
          "GNFR_area_sources","GNFR_area_sources","GNFR_area_sources",
          "GNFR_area_sources","GNFR_area_sources","GNFR_area_sources",
          "GNFR_area_sources","GNFR_area_sources","GNFR_area_sources",
          "GNFR_area_sources","GNFR_area_sources","GNFR_area_sources",
25          "GNFR_area_sources"
/
.
```

S4 COSMO-ART example namelist INPUT_OAE

```

&OAECTL
  in_tracers = 1,
/
5 &TRACER
  yshort_name = 'NO2',
  ycat1 =      'NOX_A_AREA', 'NOX_A_POINT', 'NOX_A_ch',
              'NOX_B_AREA', 'NOX_B_POINT', 'NOX_B_ch',
              'NOX_C_AREA', 'NOX_C_ch',
10            'NOX_D_AREA', 'NOX_D_POINT', 'NOX_D_ch',
              'NOX_E_AREA', 'NOX_E_ch',
              'NOX_F_AREA', 'NOX_F_ch',
              'NOX_G_AREA', 'NOX_G_ch',
              'NOX_H_AREA', 'NOX_H_POINT', 'NOX_H_ch',
15            'NOX_I_AREA', 'NOX_I_ch',
              'NOX_J_AREA', 'NOX_J_POINT', 'NOX_J_ch',
              'NOX_K_AREA', 'NOX_K_ch',
              'NOX_L_AREA', 'NOX_L_ch',
  ytpl =      'GNFR_A_EU', 'GNFR_A_EU', 'GNFR_A_CH',
20            'GNFR_B_EU', 'GNFR_B_EU', 'GNFR_B_CH',
              'GNFR_C_EU', 'GNFR_C_CH',
              'GNFR_D_EU', 'GNFR_D_EU', 'GNFR_D_CH',
              'GNFR_E_EU', 'GNFR_E_CH',
              'GNFR_F_EU', 'GNFR_F_CH',
25            'GNFR_G_EU', 'GNFR_G_CH',
              'GNFR_H_EU', 'GNFR_H_EU', 'GNFR_H_CH',
              'GNFR_I_EU', 'GNFR_I_CH',
              'GNFR_J_EU', 'GNFR_J_EU', 'GNFR_J_CH',
              'GNFR_K_EU', 'GNFR_K_CH',
30            'GNFR_L_EU', 'GNFR_L_CH',
  yvpl =      "GNFR_area_sources", 'GNFR_A', "GNFR_area_sources",
              "GNFR_area_sources", 'GNFR_B', "GNFR_area_sources",
              "GNFR_area_sources", "GNFR_area_sources",
              "GNFR_area_sources", 'GNFR_D', "GNFR_area_sources",
35            "GNFR_area_sources", "GNFR_area_sources",
              "GNFR_area_sources", "GNFR_area_sources",
              "GNFR_area_sources", "GNFR_area_sources",
              "GNFR_area_sources", 'GNFR_H', "GNFR_area_sources",
              "GNFR_area_sources", "GNFR_area_sources",
40            "GNFR_area_sources", 'GNFR_J', "GNFR_area_sources",
              "GNFR_area_sources", "GNFR_area_sources",
              "GNFR_area_sources", "GNFR_area_sources",
  contribl = 0.18, 0.18, 0.18,
45            0.18, 0.18, 0.18,
              0.18, 0.18,
              0.18, 0.18, 0.18,
              0.18, 0.18,

```

5

/
.

0.18, 0.18,
0.18, 0.18,
0.18, 0.18, 0.18,
0.18, 0.18,
0.18, 0.18, 0.18,
0.18, 0.18,
0.18, 0.18,

S5 COSMO-ART comparison online vs. offline

Fig. S1 shows averaged relative differences between the online and offline simulation for several COSMO-ART output variables. The differences are calculated for the lowest model layer and the averaging is done in the following way:

$$DIFF = \left| \frac{2 \times (\bar{\phi}_{\text{online}} - \bar{\phi}_{\text{offline}})}{\bar{\phi}_{\text{online}} + \bar{\phi}_{\text{offline}}} \right|, \quad (1)$$

5 where the spatially averaged field $\bar{\phi}$ is

$$\bar{\phi} = \frac{1}{N_i N_j} \sum_{i=1}^{N_i} \sum_{j=1}^{N_j} \phi_{i,j}. \quad (2)$$

Here, i and j are the grid indices in zonal and meridional directions, respectively. N_i and N_j are the total number of grid points in both directions and $\phi_{i,j}$ is the grid-point value of the respective variable.

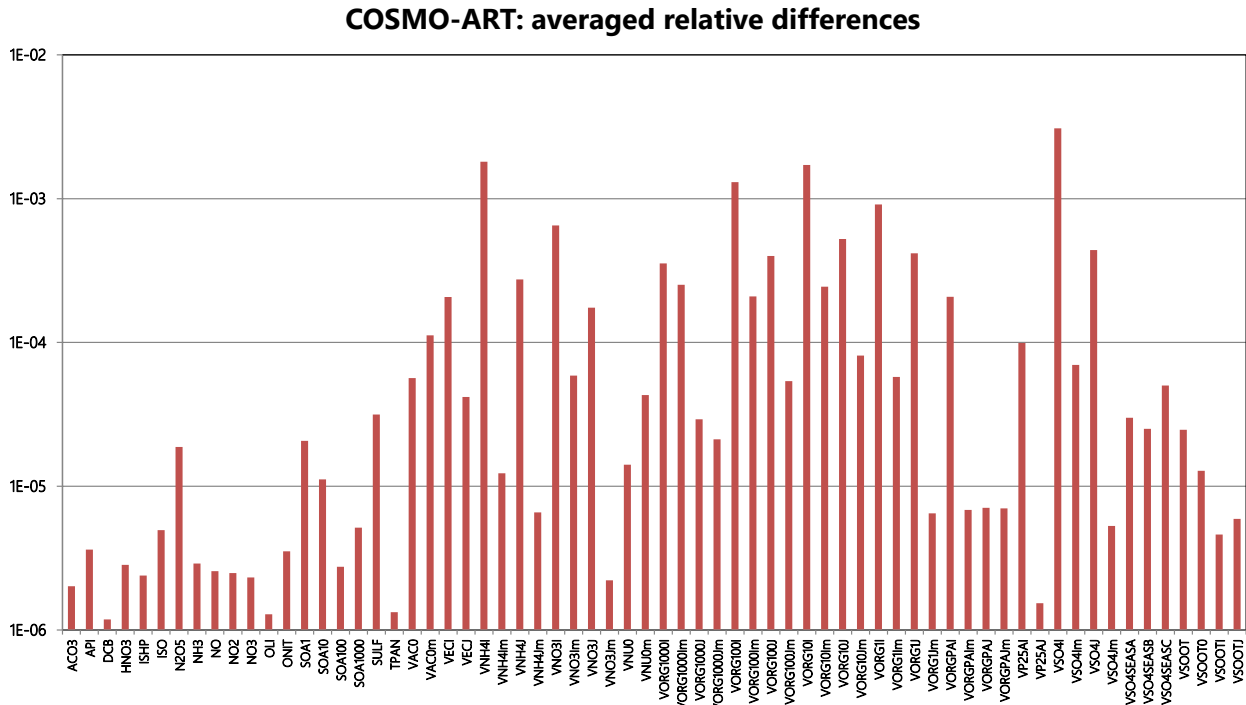


Figure S1. Averaged relative differences of COSMO-ART chemical species with values greater than 10^{-6} . Species starting with a "V" are aerosol compounds.

References

- Bieser, J., Aulinger, A., Matthias, V., Quante, M., and van Der Gon, H. D.: Vertical emission profiles for Europe based on plume rise calculations, *Environmental Pollution*, 159, 2935–2946, <https://doi.org/10.1016/j.envpol.2011.04.030>, <http://www.sciencedirect.com/science/article/pii/S0269749111002387>, 2011.
- 5 Brunner, D., Kuhlmann, G., Marshall, J., Clément, V., Fuhrer, O., Broquet, G., Löscher, A., and Meijer, Y.: Accounting for the vertical distribution of emissions in atmospheric CO₂ simulations, *Atmospheric Chemistry and Physics*, 19, 4541–4559, <https://doi.org/10.5194/acp-19-4541-2019>, <https://www.atmos-chem-phys.net/19/4541/2019/>, 2019.
- Denier van der Gon, H., Hendriks, C., Kuenen, J., Segers, A., and Visschedijk, A.: Description of current temporal emission patterns and sensitivity of predicted AQ for temporal emission patterns: TNO Report, EU FP7 MACC deliverable report D_D-EMIS_1.3, Report, MEP-R2003/166, Apeldoorn, The Netherlands, 2011.
- 10 Haussaire, J.-M., Brunner, D., Marshall, J., Prunet, P., Augusti-Panareda, A., Manders, A., Segers, A., Denier van der Gon, H., Maenhout, G., Houweling, S., and Krol, M.: CHE Deliverable 2.1 - Model systems and simulation configurations, Version 2.0, Tech. rep., CO₂ Human Emissions Project, <https://www.che-project.eu/sites/default/files/2018-04/CHE-D2-1-V2-0.pdf>, 2018.
- 15 Pouliot, G., Pierce, T., van der Gon, H. D., Schaap, M., Moran, M., and Nopmongcol, U.: Comparing emission inventories and model-ready emission datasets between Europe and North America for the AQMEII project, *Atmospheric Environment*, 53, 4 – 14, <https://doi.org/https://doi.org/10.1016/j.atmosenv.2011.12.041>, <http://www.sciencedirect.com/science/article/pii/S1352231011013288>, 2012.